J. Physiol. (1986), **370**, *pp.* 651–678
With 12 text-figures
Printed in Great Britain

ELECTROPHYSIOLOGICAL PROPERTIES OF NEONATAL RAT MOTONEURONES STUDIED *IN VITRO*

BY BARBARA P. FULTON* AND KERRY WALTON†

From the †Department of Physiology and Biophysics, New York University Medical Center, 550 First Avenue, New York, NY 10016, U.S.A. and Department of Biophysics, University College London, Gower Street, London, WC1E 6BT

(*Received 9 January 1985*)

SUMMARY

1. The electroresponsive properties of neonatal lumbar spinal motoneurones were studied using isolated, hemisected spinal cords from neonatal rats aged 3–12 days. The extracellular and intracellular responses to electrical stimulation of the ventral and dorsal root were studied as well as the intracellular response to current injection.

2. Field potentials recorded in the lateral motor area following electrical stimulation of lumbar ventral roots had a triphasic positive–negative–positive wave form. The negative component did not return to the base line smoothly but exhibited a 'shoulder' where the negativity increased in duration. Following electrical stimulation of the dorsal root, presynaptic field potentials were recorded upon activation of the afferent axons as well as following synaptic activation of interneurones and motoneurones.

3. The input resistances of neonatal motoneurones determined from the slope of current–voltage plots were high compared with the adult. The resistance decreased with age with a mean of 18·1 MΩ for animals 3–5 days old, 8·8 MΩ for animals 6–8 days old and 5·4 MΩ for animals 9–11 days old. Values for the membrane time constant were similar to those in the adult with a mean of 4·5 ms.

4. Action potentials elicited by ventral or dorsal root stimulation or by intracellular current injection were marked by a pronounced after-depolarization (a.d.p.) and an after-hyperpolarization (a.h.p.). The amplitude of the a.h.p. varied with that of the a.d.p.

5. The amplitude of excitatory post-synaptic potentials (e.p.s.p.s) elicited by electrical stimulation of the dorsal root was affected by intracellular current injection. Two types of e.p.s.p.s were distinguished: those with a biphasic reversal (early phase first) and those in which the early phase was unaffected by inward current injection while the later phase was reversed. Unlike in the adult, the reversals could be achieved with low current levels and the amplitude of both types of e.p.s.p. was increased by inward current injection.

* Present address: Department of Zoology, University College London, Gower Street, London, WC1E 6BT.

† To whom correspondence should be sent.

6. Inhibitory post-synaptic potentials (i.p.s.p.s) were elicited by dorsal or ventral root stimulation. The amplitude of these i.p.s.p.s was diminished and reversed in sign with inward current injection and their amplitude was enhanced with outward current injection.

7. Activation of neonatal motoneurones with long current pulses revealed that there is one steady-state firing range. The firing properties of neonatal motoneurones differ from those of adult rat in that (a) there is no clear threshold for repetitive firing, (b) there is a low maximum firing frequency (near 30 Hz) and (c) the slope of the firing frequency–injected current (f–I) plot has a high gain.

8. These results are discussed with respect to previous findings in adult rat and cat and with reference to the properties of the developing nervous and muscular systems.

INTRODUCTION

The electrophysiological properties of single mammalian central neurones were first investigated intracellularly in cat spinal motoneurones by Brock, Coombs & Eccles (1952). Since then a large literature has amassed regarding the anatomical (see Conradi, 1976) and physiological (see Burke & Rudomin, 1977) properties of these cells. Nevertheless, *in vivo* studies of the mammalian spinal cord do have certain shortcomings. Perhaps the greatest of these is that neither the ionic environment nor the application of pharmacological agents can be precisely controlled. To overcome these problems a number of isolated mammalian spinal cord preparations have recently been developed (Takahashi, 1978; Saito, 1979; Bagust & Kerkut, 1981; Shapovalov, Shiriaev & Tamarova, 1981; Fulton, 1983). Of these the hemisected spinal cord of the neonatal rat, introduced by Otsuka & Konishi in 1974 survives particularly well *in vitro*.

The properties of immature cat motoneurones have, with one exception (Shapovalov *et al.* 1981), been studied *in vivo*. Thus, very few intracellular investigations of the electrophysiological and biophysical characteristics of neonatal or adult motoneurones have been carried out in which the advantages of an isolated preparation have been exploited.

In this paper we report the findings of an investigation of the electrophysiological properties of lumbar motoneurones determined by intracellular recording and by means of field potential analysis in the isolated, hemisected spinal cord of the neonatal rat. A study of the ionic mechanisms underlying the properties of these cells has also been carried out (Walton & Fulton, 1985). This work has appeared in abstract form (Fulton & Walton, 1981; Walton & Fulton, 1981).

METHODS

Spinal cord dissection

Experiments were carried out using spinal cords isolated from neonatal rats 3–12 days old (Otsuka & Konishi, 1974). After isolation (carried out in bathing medium kept at 5–10 °C) a hemicord was pinned with the medial surface uppermost on a layer of Sylgard resin in the central compartment of the four-compartment recording chamber (see Llinás & Sugimori, 1980) and continually superfused with saline equilibrated with O_2/CO_2 (95 %/5 %). Most experiments were begun after about 60 min when the preparation had reached room temperature (20–25 °C) and was equilibrated

with the superfusion solution. The hemicord was transilluminated and viewed using a dissecting microscope.

Saline and drugs

The spinal cord was superfused with a modified Krebs saline which contained 113 mM-NaCl; 4·5 mM-KCl; 1 mM-$MgSO_4$; 2 mM-$CaCl_2$; 11 mM-glucose and was buffered to pH 7·2 with 1·0 mM-Na_2HPO_4 and 25 mM-$NaHCO_3$. Hydrogen peroxide was added to all solutions at 0·003% (Llinás & Sugimori, 1980; Walton & Fulton, 1983). In some experiments mephenesin (1 mM) was added to block polysynaptic activity (Wright, 1954).

Stimulation and recording

Antidromic and synaptic activation of the cells were achieved using suction electrodes placed on the ventral and dorsal roots respectively (Fig. 1). We used segments L4–L6 which correspond to L6–S2 in the cat. In the youngest animals, in which the roots are very fine, more than one root was held in each suction electrode. A switch allowed the ventral root suction electrode to be used either for recording the spinal reflex or for antidromic activation of motoneurones. In some experiments a pair of silver wires was used to record the dorsal root volley as it entered the spinal cord.

The extracellular recordings of field potentials were obtained by means of glass micropipettes filled with 2 M-NaCl and with a d.c. resistance of 5–20 MΩ. In these experiments a thin layer of agar was placed beneath the spinal cord to allow the micro-electrode to be lowered completely through the cord without breaking the tip. Records were taken at 100 μm intervals beginning at the bottom of each track to avoid tissue distortion during electrode penetration. For intracellular recording glass micropipettes with an average d.c. resistance of 55–65 MΩ were used. These were filled with 3 M-K chloride, 2 M-K citrate, or 3 M-K acetate. Direct activation of impaled motoneurones was implemented using a high-impedance (10^{11} Ω) bridge amplifier (Neurodata IR 283D). Capacity compensation allowed frequency responses of 10–15 kHz, depending on the micro-electrode characteristics. Only motoneurones with stable resting potentials of −60 mV or more are included in this study (Table 1). The data base for these experiments consists of records from more than 300 motoneurones. Data were photographed directly from the oscilloscope screen or stored on magnetic tape or on floppy disks. A Nicolet 4090-2 digital oscilloscope was used for averaging field and synaptic potentials and for artifact subtraction. The data were displayed on a Tektronix 611 oscilloscope and printed using a hard copy unit.

Histological processing

Under ether anaesthesia animals were perfused intracardially with buffered formaldehyde fixative (5% formaldehyde, 5% dextrose in phosphate buffer) for 30 min. The spinal cords were removed and post-fixed for 24 h. The tissue was then dehydrated through a series of alcohols, embedded in epoxy resin and sections cut and stained with Cresyl Violet.

RESULTS

Spinal reflex

The viability of the preparation was assessed at the beginning of each experiment by electrical stimulation of the dorsal roots and recording (i) the incoming dorsal root volley; (ii) the arrival of the afferent volley in the ventral horn, as determined by the presence of an orthodromic field potential, and (iii) the amplitude and time course of a spinal reflex recorded from the ventral roots (Fig. 1). Typically the reflex had two components, a fast rising positive–negative response generated by the monosynaptic reflex pathway, followed by a second slower, small positivity representing polysynaptic activity (Fig. 1). This configuration is very similar to the potentials recorded in late fetal (Saito, 1979) and new-born rats (Otsuka & Konishi, 1974) and adult cat (Renshaw, 1940). Immediately following the dissection, the monosynaptic

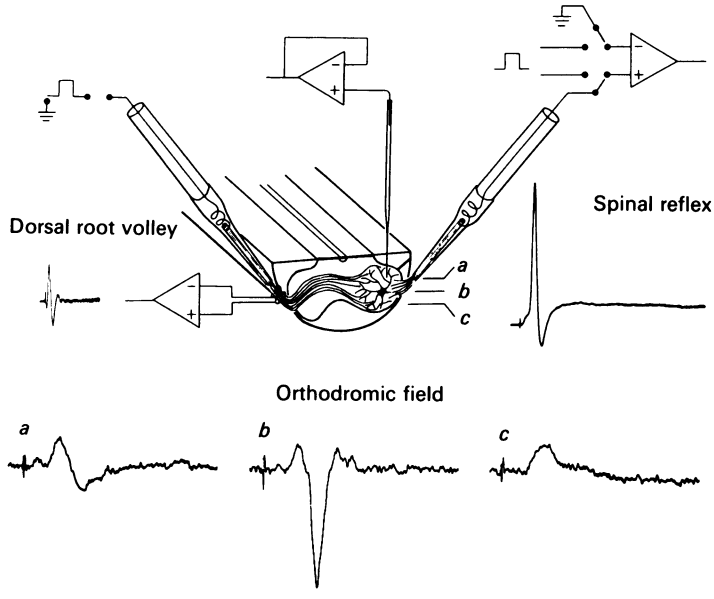

Fig. 1. Diagram of the spinal cord and arrangement of recording and stimulating electrodes. Stimulation of roots was achieved using a suction electrode. The dorsal root volley was monitored using a pair of Ag–AgCl wires (top left). Extracellular field potentials due to synaptic activation of motoneurones were recorded above (*a*), at the level of (*b*), and below (*c*) the motoneurone somata (bottom). The spinal reflex was recorded using a suction electrode (top right). A switch (upper right) allowed the same electrode to be used for antidromic stimulation and recording the spinal reflex (the polarity of the recordings is positive upwards).

component of the reflex was usually 2–4 mV, but improved reaching a stable value of 4–12 mV after 30–45 min.

Field potentials

The behaviour of specific neuronal populations was tested by recording the field potentials following supramaximal ventral or dorsal root stimulation. Ventral root stimulation was usually repeated at a maximum rate of 1 Hz. The dorsal root stimulus frequency was usually 0·2 or 0·1 Hz, since the response amplitude decremented at higher rates. The extracellular field potentials, illustrated in Figs. 2–5, were obtained from a 7-day-old rat. A drawing of a transverse section through the lumbar cord (Fig. 2*A*) illustrates the orientation of the spinal cord during the experiments and gives the approximate location of the twelve electrode tracks (100 μm apart). In order to facilitate comparison with *in vivo* studies, however, the results of the field potential study are presented with the spinal cord oriented with the dorsal surface uppermost (Figs. 2, 4 and 5). Each recording shown in Figs. 2–4 is the average of twenty individual responses.

Antidromic fields. The response to ventral root stimulation as seen in the ventral horn (Fig. 2*B*) consisted of a triphasic positive–negative–positive wave form typical of action potential propagation in volume conductors (Lorente de No, 1947). The

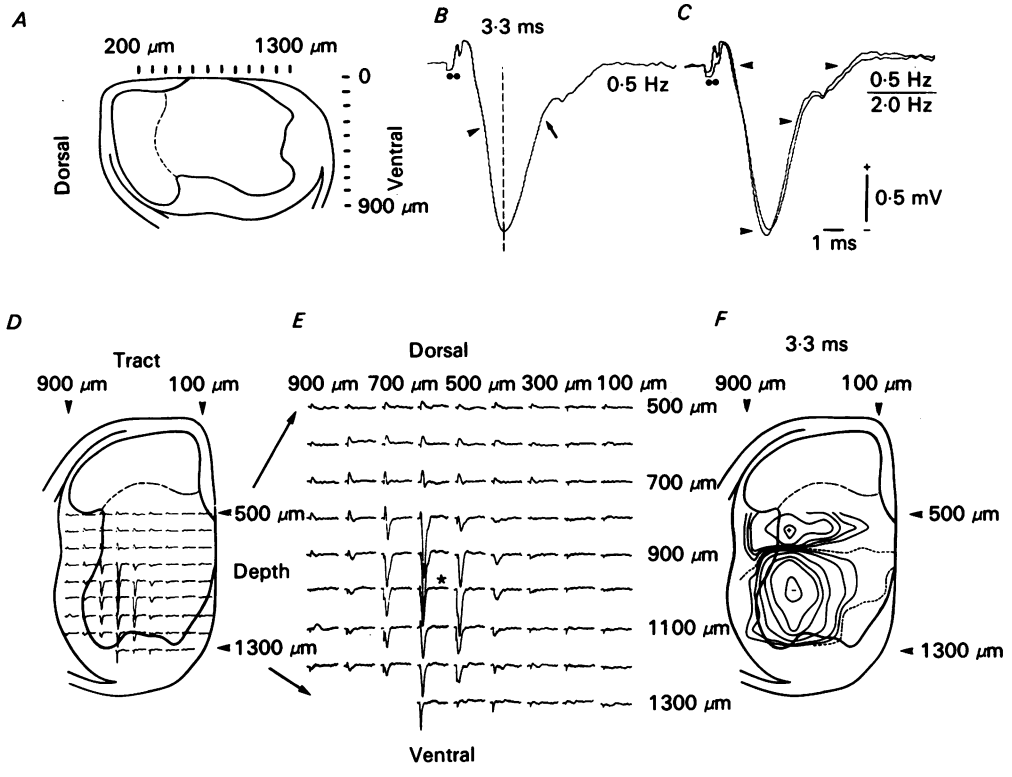

Fig. 2. Extracelluar field potentials elicited by ventral root stimulation. *A*, drawing of a coronal section of hemisected spinal cord is positioned as during the experiment. Twelve tracks were recorded at 100 μm intervals (200–1300 μm). Recordings were made every 100 μm from the bottom of each track (900 μm) to the surface (0 μm). *B*, response in the ventral horn (track 500 μm, depth 700 μm) to ventral root stimulation at 0·5 Hz. *C*, superposition of responses to 0·5 Hz and 2 Hz (arrowheads) stimulation. (Dots in *B* and *C* indicate stimulus artifact.) *D*, outline of the hemicord oriented as *in situ* with the dorsal surface up. Potentials recorded in tracks 100–900 μm from the mid-sagittal surface for depths of 500–1300 μm from the dorsal surface are illustrated. *E*, field potentials in *D* are shown enlarged. Note that the field is restricted to the ventrolateral cord. Each trace is the average of twenty consecutive responses, * indicates response displayed at one-half of the gain of the other traces. *F*, isopotential lines giving the amplitude of the field recorded at 3·3 ms from stimulus artifact (*B*), (lines represent +0·2, +0·15, +0·1, +0·075, +0·05, −1·5, −0·75, −0·5, −0·25, −0·1, −0·05 mV), dashed line gives the zero isopotential. Each trace is the average of twenty consecutive responses. At 0·5 Hz the first ten responses were not recorded (7-day-old animal).

initial positivity was sometimes obscured by the stimulus artifact and the presence of the second positivity depended on the location of the recording electrode (Nelson & Frank, 1964). The break in the rising phase of the field (arrowhead, Fig. 2*B*) corresponds to the break between the initial segment (i.s.) and somadendritic (s.d.) components of the intracellular action potentials recorded during antidromic invasion (see below). A negative 'shoulder' was sometimes seen on the return phase of the negativity (arrow, Fig. 2*B*). When the ventral root was stimulated at a higher

frequency, i.e. 2 Hz (arrowheads, Fig. 2*C*), the initial positivity was unaffected while the negative component became slightly larger and narrower. It can also be seen that the shoulder on the negativity had a lower amplitude and that the second positivity was increased somewhat in amplitude. By contrast, dorsal root stimulation at 2 Hz produced marked changes in field potential configuration (see below). The wave forms

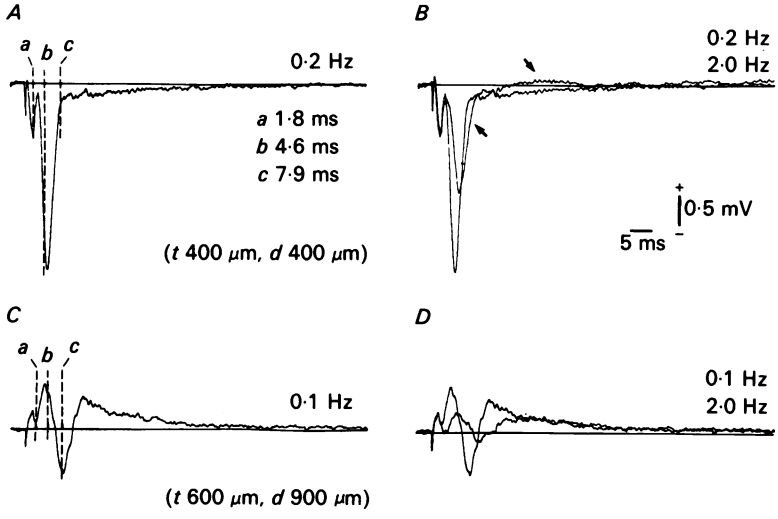

Fig. 3. Extracellular field potentials elicited by dorsal root stimulation. *A* and *B*, recordings obtained in a track 400 μm from the mid-sagittal surface at a depth of 400 μm. *A*, at a stimulus frequency of 0·2 Hz, the response consisted of a sharp positive–negative–positive wave form followed by a large negativity and a prolonged, low amplitude negativity. *B*, at high frequency stimulation (2 Hz, arrows) there was no change in the early triphasic response but the latency of the large amplitude negativity increased as its amplitude decreased; the late negativity became positive. *C* and *D*, recordings obtained from the region of the lateral motor area. *C*, at 0·1 Hz stimulation a small positivity was followed by a triphasic (positive–negative–positive) response which returned slowly to the base line. *D*, at 2 Hz the triphasic portion of the wave form was smaller and had an increased latency, the return to base line is unaffected. Each trace is the average of twenty consecutive responses. At 2 Hz stimulation, the first ten responses were not included in the average. (Same animal as in Fig. 4.)

recorded following ventral root stimulation and their distribution relative to the outline of the hemicord in coronal section are shown in Fig. 2*D* and *E*. Note that the large negativity is restricted to the lateral motor area and is followed by a low amplitude positive wave at some recording points, e.g. tracks 500 and 600 μm. The spatial distribution and polarity of the antidromic field potential reflects the activation of motoneurone somata and the spread of potential into the dendrites (Nelson & Frank, 1964). Note that the potentials displaying the most prominent shoulder on the negativity are found at depths of 700 and 800 μm. Further below an early sharp negativity was recorded near the ventral edge of the field, where the motoneurone axons leave the cord, reflecting the antidromic volley of these axons.

The amplitude of the field 3·3 ms after the stimulus artifact has been reconstructed

in Fig. 2*F*, and is illustrated as isopotential lines with the zero isopotential given by the dashed line. This pattern is typical of a closed field (Lorente de No, 1947). Although the true current sinks and sources cannot be identified accurately from this type of data (Pitts, 1952), Fig. 2*F* does indicate that there is one current sink in the lateral motor area. The most prominent current source is dorsal to this where the largest positivity was typically recorded.

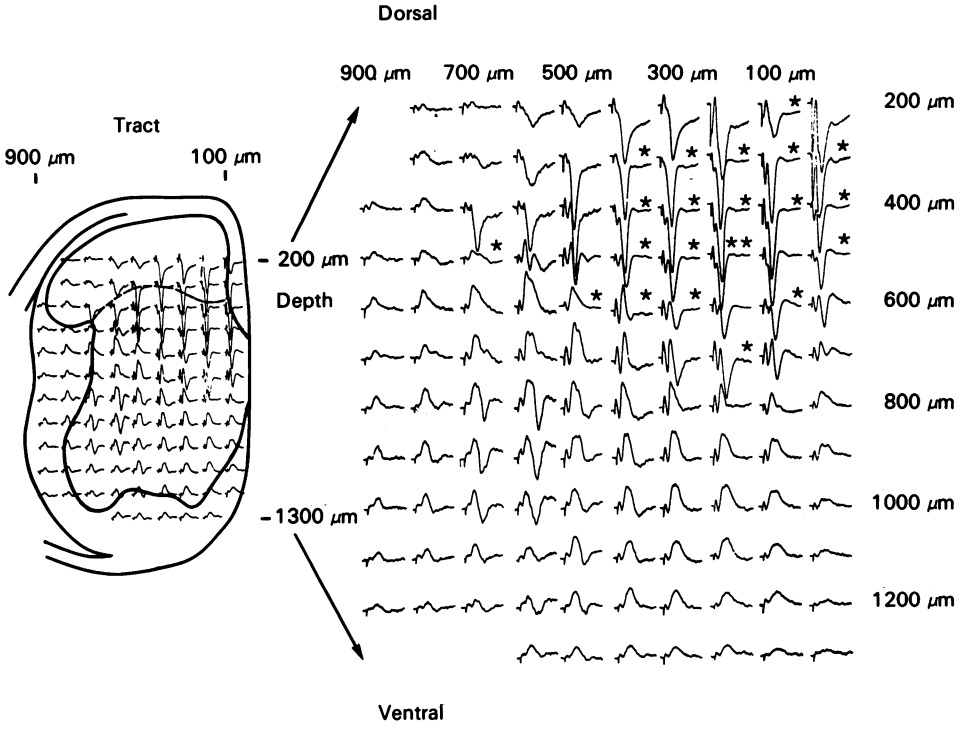

Fig. 4. Distribution of extracellular field potentials recorded after dorsal root stimulation. Insert gives the approximate location of the recording sites. Potentials were recorded at 100 μm intervals from the mid-sagittal surface to 700 μm or 900 μm, beginning 200 μm from the dorsal surface to a depth of 1300 μm. Potentials recorded in the dorsomedial portion of the cord are dominated by a large negativity which reversed near 500–600 μm in depth. Activation of the motoneurones is seen in the triphasic response in the ventrolateral portion of the hemicord. All traces are the average of twenty consecutive responses, * indicates a response displayed at one-half gain, ** a response at one-third gain. (Same animal as in Fig. 3.)

Orthodromic fields. Two major areas of extracellular activity were identified following dorsal root stimulation, one in the dorsal and one in the ventral cord. This pattern is similar to that seen in adult cat (Eccles, Fatt, Landgren & Winsbury, 1954). Recordings typical of these locations are illustrated in Fig. 3. In the dorsal spinal cord (track (*t*) 400 μm, depth (*d*) 400 μm) (Fig. 3*A* and *B*) the response to 0·2 Hz stimulation consisted of an early triphasic positive–negative–positive wave form followed by a large, sharp negativity and a prolonged negativity which returned the potential slowly to the base line. The components of this field potential are dissected

by comparing the responses to 0·2 and 2 Hz (arrows) stimulation (Fig. 3*B*). At 2 Hz the early triphasic response was unaffected but the large negativity decreased in amplitude and showed a decreased rate of rise. At this location the slow negativity changed in sign and became positive, but at other locations, where this component was more prominent (e.g. *t* 100 μm, *d* 300 μm), 2 Hz stimulation diminished, but did

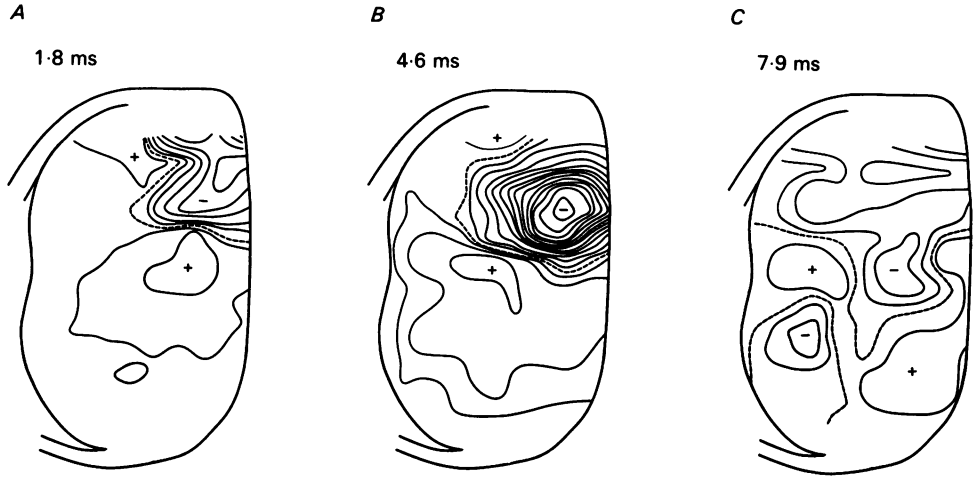

Fig. 5. Isopotential lines showing amplitude of response to dorsal root stimulation at three times after the stimulus; data from Fig. 4. *A*, field at 1·8 ms reflects the arrival of the afferent volley in the dorsal cord. Lines represent −1, −0·75, −0·5, −0·25, −0·1 and +0·25, +0·1 mV. *B*, at 4·6 ms a negativity in the region of the interneurones dominates. Lines represent −3·0 to −0·25 mV in steps of 0·25, −0·1, +0·25 and +0·1 mV. *C*, response at 7·9 ms, corresponds to activation of the motoneurone somata. Lines represent −0·5, −0·25, −0·1 and +0·25, +0·1 mV; dashed lines give zero isopotentials (same animal as in Fig. 3). (See text for details.)

not reverse this component. While it is difficult to interpret unambiguously the orthodromic field potential wave forms in terms of the current flow in single cells, work on single cell extracellular fields (Nelson & Frank, 1964), suggests that the early triphasic wave form reflects the incoming volley in the dorsal root axons and the later components reflect post-synaptic events (Eccles *et al.* 1954).

In the ventral cord (e.g. *t* 600 μm, *d* 900 μm) (Fig. 3*C* and *D*), following stimulation at 0·1 Hz, a small positivity was followed by a triphasic (positive–negative–positive) wave form (Fig. 3*C*). The last positivity was quite prolonged. With 2 Hz stimulation the early positivity was unchanged, but the amplitude of the triphasic component was smaller and demonstrated an increased latency (Fig. 3*D*). The slow return of the positivity to the base line was unaffected, however. These changes indicate that the triphasic response reflects synaptic activation and spike initiation in motoneurones.

The distribution of the extracellular response to dorsal root stimulation within the hemicord is shown in Fig. 4. The wave form recorded in the dorsomedial part of the cord resembles that shown in Fig. 3*A*. The large amplitude negativity was the most prominent feature and has consistently been the largest component recorded from the neonatal animals. This component reversed in sign at progressively deeper levels

from the lateral to the medial aspect of the cord and was so large that it dominated the response recorded at the same time in the ventromedial cord.

In the lateral motor region of the hemicord the triphasic wave form illustrated in Fig. 3*C* predominated, the negative component being limited to that region containing motoneurone somata. However, the positivity serving as a current sink for this component could not be isolated from the positivity corresponding to the large sink in the dorsomedial hemicord. These records make it very clear (more so in fact than in adult spinal cord) that the sources and sinks throughout the entire tissue contribute to the wave form recorded at each point (Pitts, 1952).

As stated above, the morphological correlates of the field potentials cannot be identified with certainty. However, to facilitate their interpretation, the amplitude of the response at three times after the dorsal root stimulus artifact was computed for each recording site and isopotential maps were constructed (Fig. 5). The times chosen were 1·8, 4·6 and 7·9 ms (*a*, *b*, *c* respectively in Fig. 3*A* and *C*). The continuous lines give the potentials in uniform increments of 0·25 mV to indicate the 'steepness' of the potential distribution. Dashed lines demark the cross-section of the zero isopotential surface. The location of the response at 1·8 ms (Fig. 5*A*) suggests that the potential is dominated by the arrival of the afferent volley in the dorsal hemicord, this is supported by the observation that this component is not changed by high frequency stimulation (Fig. 3*B*). At 4·6 ms (Fig. 5*B*) a large negative field is seen to be restricted to the dorsomedial and intermediate zones. Due to its location and susceptibility to repetitive stimulation (Fig. 3*B*) this response probably reflects synaptic activation of interneurones. At 7·9 ms (Fig. 5*C*) the distribution of potential is more diffuse and difficult to interpret. There are two current sinks, one in the lateral motor area (probably representing the synaptic activation of motoneuronal somata) and one ventral to the intermediate–dorsomedial zone which extends dorsally; this may reflect a late current sink in the interneurones. Two areas of positivity separate these serving as sources for both regions and cannot be interpreted further. Taken together these three plots illustrate the spread of activity through the spinal cord from the entry of the dorsal root volley (Fig. 5*A*), to activation of the neurones in the intermediate zone (Fig. 5*B*) to activation of the motoneurones (Fig. 5*C*). A late (20–25 ms), prolonged (45–50 ms) negative response was also seen in the dorsal cord.

Identification of motoneurones

The peak amplitude of the negative antidromic field potential was used to locate the motoneurone pool within the ventral horn; the exact location depended on the age of the animal. As the micro-electrode was lowered into the hemicord, the ventral roots were stimulated at 2 Hz. Proximity to individual motoneurones was marked by a decrease in the width and an increase in the amplitude of the negative component of the extracellular field potential. Cells which produced an antidromic action potential upon penetration were identified as motoneurones. When filled with Lucifer Yellow such cells were found to send their axon into a ventral root. In the course of locating motoneurones we often penetrated electrically inexcitable cells with large resting potentials (about −80 mV) and low input resistances. As has been suggested in studies of cat spinal cord (Coombs, Eccles & Fatt, 1955), these cells appear to be glia since when such a cell was filled with Lucifer Yellow, many small, closely packed

cells were seen to be filled with dye. This finding is not surprising as glial cells have long been known to be connected through low resistance bridges and recently glial cells in neocortical slices have been shown to be dye coupled.

Passive membrane properties

The passive properties of neonatal motoneurones were determined by passing short (100 ms), low amplitude current pulses through the recording electrode (Fig. 6*A*).

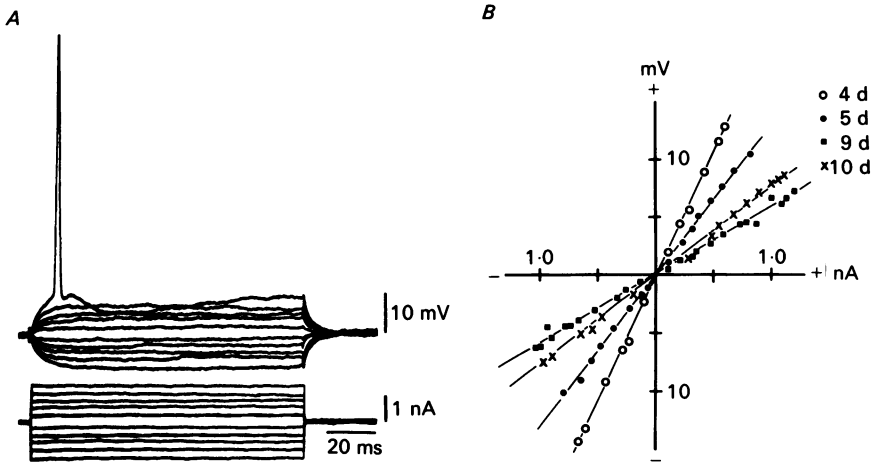

Fig. 6. Passive membrane properties of neonatal motoneurones. *A*, response of 9 day motoneurone to current pulses. Note that there is no anomalous rectification at these current levels. *B*, current–voltage plot of responses of motoneurones of 4, 5, 9, and 10-day-old animals. The slope resistances are 23 MΩ (4 day), 10 MΩ (5 day), 2·5 MΩ (9 day) and 4 MΩ (10 day). The current–voltage relation is linear in every case.

Current–voltage plots were linear for voltages between the resting potential and spike threshold. Four examples are shown in Fig. 6*B*. In the small range of hyperpolarizing currents examined no anomalous rectification was seen. Although this is in agreement with an early study in adult cat motoneurones *in vivo* (Coombs *et al.* 1955), a non-linear change in membrane resistance with hyperpolarization has been reported in some motoneurones (Nelson & Frank, 1967). The apparent input resistance, as determined from the slope of the current–voltage plots, varied with age (see Table 1), with mean values of 18·1 MΩ (S.D. = ±7·0 MΩ, $n = 18$) at 3–5 days, 8·8 MΩ (S.D. = ±5·1 MΩ, $n = 10$) at 6–8 days, and 5·4 MΩ (S.D. = ±1·7 MΩ, $n = 12$) at 9–11 days. This decrease in resistance with age is most likely due to the growth of the cells during this period of development (Mellstrom & Skoglund, 1969; Conradi, 1976). We have examined Cresyl-Violet-stained coronal sections of a small sample of spinal cord from rats of different post-natal ages. We found the mean diameter of lumbar motoneurones based on measurements of two diameters at right angles in a nucleolar section to be 16·9 μm (S.D. = ±1·9 μm, $n = 39$) at 1 day, 19·6 μm (S.D. = ±2·0 μm, $n = 35$) at 5 days and 23·3 μm (S.D. = ±2·5 μm, $n = 59$) at 9 days. Allowing for shrinkage of 20 % (Mellstrom & Skoglund, 1969) this would give values of 21·1, 24·5 and 29·1 μm, respectively.

TABLE 1. Values for resting potential, spike height, width, duration of a.h.p. and input resistance (R_{in}) for post-natal ages 3–12 days

Age (days)	Resting potential (mV)	Spike			R_{in} (MΩ)
		Amplitude (mV)	Width (ms)	A.h.p. duration (ms)	
3	60	71	1·7	140	23·0
3	60	66	1·7	86	12·0
3	60	64	1·6	104	—
3	61	66	3·0	—	7·7
3	61	84	2·7	135	15·4
4	65	83	1·3	113	16·2
4	67	90	1·1	104	9·8
4	60	74	1·7	130	37·5
4	75	80	2·6	178	20·5
4	73	97	1·3	108	23·0
5	61	80	1·3	116	12·9
5	63	68	1·9	100	21·2
5	60	79	1·3	104	13·8
5	75	86	1·3	103	20·7
5	69	74	1·7	113	10·0
6	69	75	1·7	120	9·8
6	66	77	1·7	153	—
6	60	68	1·3	108	13·2
6	60	79	1·6	78	14·2
6	74	82	1·6	159	18·8
7	67	77	1·5	129	—
7	67	71	1·5	108	—
7	60	67	1·8	—	10·0
7	71	90	1·7	—	7·9
8	66	75	1·3	120	12·4
8	81	102	1·1	108	—
8	67	70	1·4	—	3·1
8	74	76	1·5	—	5·7
8	60	72	1·3	108	4·9
9	63	71	1·7	—	6·0
9	60	78	1·3	—	2·5
9	60	74	1·3	—	4·2
9	60	72	1·5	141	6·9
9	68	73	1·2	106	4·5
10	71	78	1·4	—	3·4
10	64	72	1·5	178	—
10	60	70	1·4	139	—
10	60	76	1·7	—	6·3
10	74	91	1·7	164	9·1
11	60	69	1·2	83	—
11	60	79	1·1	87	—
11	65	84	1·7	—	5·6
12	60	68	1·5	122	—
12	65	78	2·0	104	—
Mean ±S.D.	64±9·2 (n = 78)	75·8±9·3 (n = 77)	1·67±0·39 (n = 77)	121·7±28 (n = 47)	

Similarly derived values for large lumbar motoneurones in adult rat have been reported to be in the range 25–50 μm (Granit, Kernell & Smith, 1963*b*). Time constants were also measured in some cells and varied between 2·3 and 6·2 ms, with a mean of 4·5 ms (S.D. = $\pm$1·4 ms, n = 7).

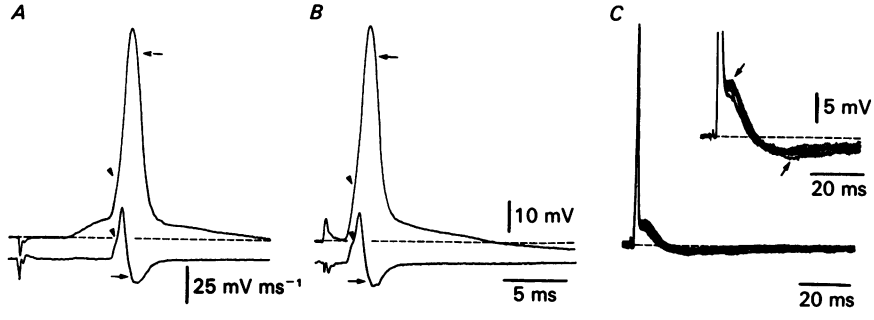

Fig. 7. Responses to dorsal and ventral root stimulation. *A*, orthodromic action potential elicited by dorsal root stimulation. Note that the spike rises from an e.p.s.p. and is followed by an a.d.p. *B*, antidromic response to ventral root stimulation. *A* and *B*, i.s.–s.d. break (arrowheads) can be seen on the rising phase of the spikes and on the time derivative of the responses (lower traces) as can a decrease in the rate of the fall of the spikes (arrows). *C*, superposition of ten consecutive responses to antidromic stimuli delivered at 1 Hz, spikes with large a.d.p.s are followed by large a.h.p.s (insert, arrows mark spike with the largest a.d.p.). (*A* and *B*, 12-day-old animal; *C*, 4-day-old animal.)

Orthodromic and antidromic action potentials

Stimulation of the dorsal roots elicited overshooting action potentials rising from an excitatory post-synaptic potential (e.p.s.p.) (Fig. 7*A*) and followed by a well-defined after-depolarization (a.d.p.) and a prolonged after-hyperpolarization (a.h.p.). The a.d.p. either took the form of a 'hump' being preceded by a 'notch' at the foot of the spike as in adult rat motoneurones (Granit *et al.* 1963*b*) or followed smoothly on the declining phase of the spike. Antidromic action potentials were elicited by ventral root stimulation (Table 1 and Fig. 7*B*). The amplitude varied between 66 and 84 mV (mean 75·8, S.D. = $\pm$9·3, n = 77), and the duration at one-half the peak amplitude between 1·1 and 3·0 ms. In contrast to observations in kitten motoneurones (Kellerth, Mellstrom & Skoglund, 1971), there was no systematic change in these parameters with age. The lower traces in Fig. 7*A* and *B* illustrate the time derivative of the spikes; here, as well as in the spikes themselves, the break between the i.s. and s.d. components (arrowheads) and a change in slope during the falling phase of the spike (arrows) are shown. The latter is due to a calcium component activated during the falling phase of the spikes (Walton & Fulton, 1985).

The a.d.p. was present in every motoneurone with an initial resting potential of at least -60 mV. This component was, however, quite labile and was often the first to be affected if the cell was injured. It was also very susceptible to membrane potential level (see below). In motoneurones that were injured upon impalement (as indicated by a low resting potential and injury discharge) the a.d.p. was often lost or became less well defined, although the spike could still be considered quite

acceptable with respect to its amplitude and rate of rise. In most cells the amplitude of the a.d.p. was remarkably constant.

Ten consecutive antidromic action potentials recorded from a cell which showed an unusually large variability in the a.d.p. and a.h.p. and some variation in the resting potential level are shown in Fig. 7*C*. In the insert of Fig. 7*C*, the rising phases of the spikes were aligned to eliminate changes in base line of the records caused by variations in the display system. Thus, while it is not the rule, substantial variability in the amplitude and shape of the a.d.p. and a.h.p. can occur in healthy motoneurones at the resting potential. This variability serves to demonstrate the relation between the a.d.p. and a.h.p., for the largest a.d.p. (insert, arrow) was followed by the largest and most prolonged a.h.p. (arrow). We found this relation between the two after-potentials to be quite consistent, suggesting that the variability in the a.h.p. is secondary to the variation in the a.d.p. This supports the finding that the conductance underlying the a.d.p. (probably calcium, see Walton & Fulton, 1981; Harada & Takahashi, 1981, 1983) triggers a significant portion of the a.h.p. through activation of a calcium-dependent potassium conductance. Despite the variability of the a.d.p. in Fig. 7*C*, it was present following every spike. This is in contrast to other reports using this preparation (Harada & Takahashi, 1983) where the a.d.p. was not always seen.

Effect of membrane potential on action potentials

The wave form of both antidromic and orthodromic action potentials varied with the resting potential level. As illustrated in Fig. 8*A* following antridromic stimulation at rest (0 nA) a fast rising spike with a clear a.d.p. and a.h.p. was recorded. When the membrane was hyperpolarized by injection of inward current (−1·21 nA), a clear i.s.–s.d. break was seen (arrow), the amplitude of the a.d.p. increased, and that of the a.h.p. decreased. With increasing hyperpolarization (−1·43 nA), the action potential failed to invade the soma and dendrites and only the i.s. component was elicited. Finally with injection of −2·68 nA only the myelinated axon (M) component remained. This sequence is identical to that reported for cat motoneurones *in vivo* (Brock, Coombs & Eccles, 1953), but less current was required to prevent both s.d. and i.s. invasion of the action potential in the neonatal cells and the critical intervals were longer than in the cat.

The effect of membrane depolarization on the antidromic action potential recorded from another motoneurone, is shown in Fig. 8*B*. With injection of 0·62 nA the i.s.–s.d. break became more apparent, and the a.d.p. was smaller and not clearly differentiated from the falling phase of the spike. At this level the a.d.p. was dominated by the conductance underlying the a.h.p. At a more depolarized level (0·87 nA), the i.s. component was present, although it had a slower rise time and lower amplitude than that recorded at the resting potential. The i.s. spike was followed by a late, small, slowly rising s.d. response and an a.h.p. Finally, at the most depolarized level (1·01 nA: Fig. 8*B*) a small amplitude i.s. component was seen. The presence of a small s.d. component is indicated by the upward deviation in the falling phase of the i.s. response and a small a.h.p. Superposition of the response obtained at 0·87 nA and the full i.s. response in this cell (obtained by hyperpolarizing the cell with 0·49 nA of current) are shown in Fig. 8*C*. The spike elicited at 0·87 nA depolarization had a

much slower rise time (due largely to sodium channel inactivation). It also had a faster rate of fall than the i.s. spike indicating a stronger activation of a potassium conductance in the s.d. compartment than in the i.s. segment under these conditions. The slow spike seen at 0·87 nA of depolarization is probably due to a s.d. conductance increase to sodium since it was still present 10 min after half of the $CaCl_2$ in the bathing solution was replaced by $CdCl_2$ (not shown).

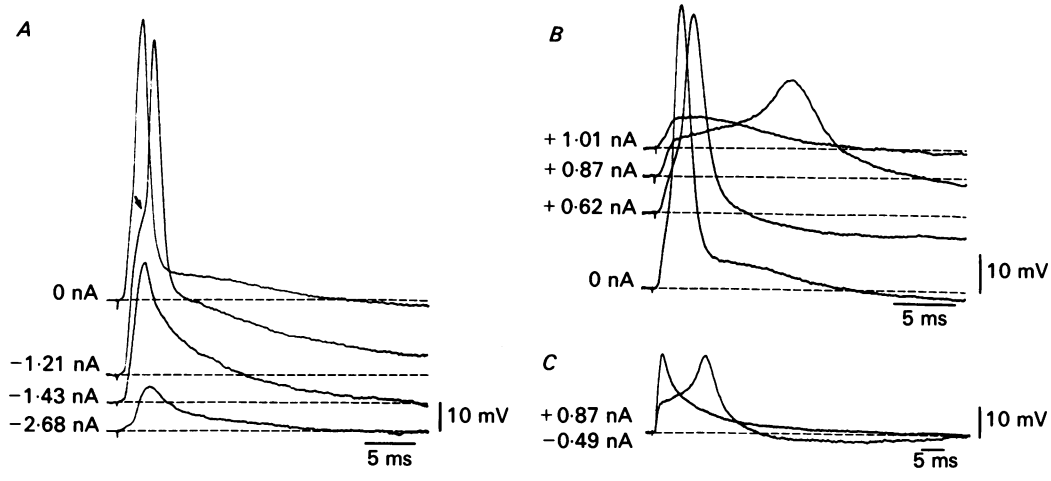

Fig. 8. Responses of neonatal motoneurones to changes in membrane potential. *A*, hyperpolarizing current injection (dashed lines give steady-state level). At rest a.d.p. and a.h.p. are present. As the cell was hyperpolarized (−1·21 nA) the i.s. and s.d. components of the spike could be clearly differentiated (arrowhead). With −1·42 nA the spike did not invade the soma and dendrites leaving the i.s. spike; at −2·86 nA invasion fails at the initial segment leaving the M spike. (Steady-state voltage levels do not reflect the membrane potential level.) *B*, depolarizing current injection. At rest the i.s.–s.d. break is apparent and there is a marked a.d.p. With +0·62 nA the rising phase of the spike is slower, the i.s.–s.d. break more pronounced and the a.d.p. dominated by the a.h.p. With an injection of +0·87 nA invasion of the soma and dendrites is hampered and a slowly rising, low amplitude spike elicited. With +1·01 nA a small depolarizing response is seen. (Steady-state voltage levels do not reflect membrane potential level.) *C*, superposition of response seen in *B* at +0·87 nA and an i.s. spike (elicited after −0·49 nA current injection); note lower gain and faster sweep speed than in *A* and *B*. (*A*, 4-day-old animal; *B*, 7-day-old animal.)

When paired stimuli were delivered at decreasing interstimulus intervals, the amplitude of the second spike gradually decreased (Brock *et al.* 1953) and the i.s.–s.d. break became increasingly apparent until with a 15 ms interval the spike failed to invade the soma, leaving only the i.s. response. The i.s. spike was lost at an 8–10 ms interval, revealing the M spike, while at shorter intervals spikes could not be elicited. As noted in adult rat motoneurones (Granit *et al.* 1963*b*), the a.d.p.s of spikes elicited by paired antidromic stimuli did not sum.

Synaptic potentials

Motoneurone spontaneous excitatory and inhibitory synaptic potentials were routinely present in our preparations. The characteristics of spontaneous inhibitory

post-synaptic potentials (i.p.s.p.s) have recently been documented by Takahashi (1984). Stimulation of the dorsal roots at increasing strengths elicited mono- and polysynaptic multifibre e.p.s.p.s which at the highest stimulus intensities were followed by a prolonged depolarizing potential. However, in the presence of 1 mM-mephenesin, which blocks polysynaptic activity (Wright, 1954) and thus largely eliminates inhibitory input, graded, monosynaptic e.p.s.p.s were recorded.

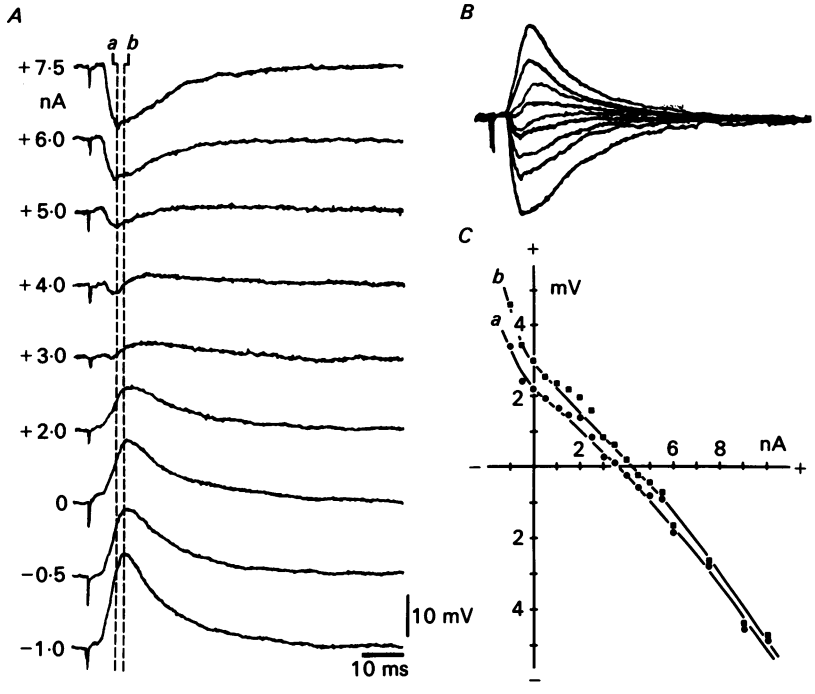

Fig. 9. Effect of current injection on multifibre e.p.s.p.s. *A*, response to dorsal root stimulation at nine current levels (given to left of trace). Each trace is the average of eight responses. Note that the rising phase of the e.p.s.p. begins to reverse at +3·0 nA and the rest of the e.p.s.p. is reversed in sign at +5·0 nA. *B*, superposition of traces shown in *A*. *C*, plot of e.p.s.p. amplitude at 6·7 ms (circles) and 8 ms (squares) after the stimulus. Note that the separation between the two lines at 0 mV is about 1 nA (7-day-old animal).

The e.p.s.p. amplitude was sensitive to intracellular current injection and grew larger as the membrane potential was made more negative (Fig. 9*A*). In cat motoneurones multifibre Ia e.p.s.p.s have been reported to be largely insensitive to injection of hyperpolarizing current (Eccles, 1957). The difference seen here may be due, in part, to the apparent lack of anomalous rectification in neonatal motoneurones. Depolarizing the cell readily decreased and completely reversed the e.p.s.p. in many cells. In the example illustrated in Fig. 9*A* the reversal of the e.p.s.p. was biphasic. The early phase started to reverse in sign at 3 nA while the remainder of the synaptic potential remained positive. With increased current (4 nA) the late portion of the synaptic potential also began to change in sign. The amplitude of the 'reversed' e.p.s.p. became larger with increasing current strength. In Fig. 9*B*

the e.p.s.p.s of Fig. 9*A* are superimposed and the changes in wave form and amplitude can be seen more clearly. The e.p.s.p. amplitude is plotted in Fig. 9*C* as a function of injected current at two times after the stimulus artifact (*a* and *b*, Fig. 9*A*). Reversal of the rising phase (*a*, circles) occurred near 3 nA and the remainder of the e.p.s.p. changed sign near 4 nA (*b*, squares) in this motoneurone (cf. Redman, 1979).

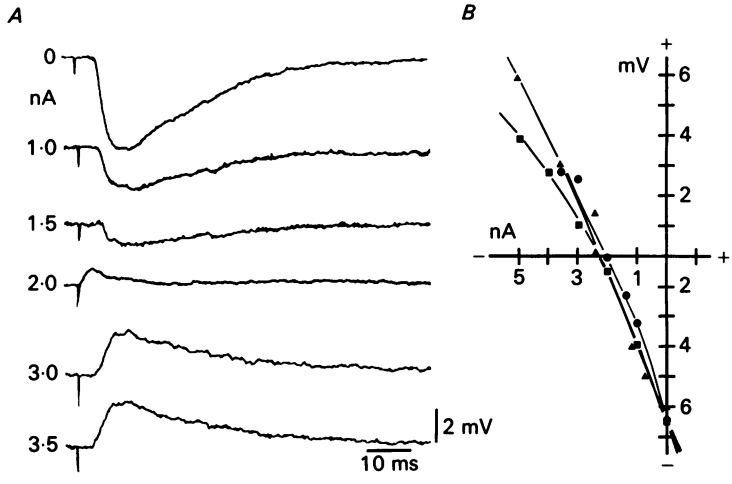

Fig. 10. Effect of current injection on i.p.s.p.s elicted by ventral root stimulation. *A*, response recorded at six current levels. Each trace is the average of eight responses. The response elicited at 2 nA, comprising largely of the intracellular record of the extracellular field potential, has been subtracted from the other responses. Note that the i.p.s.p. reverses sign monophasically. *B*, plot of the amplitude of the i.p.s.p. as a function of injected current. The results of three trials in the same cell are plotted. The reversal of this i.p.s.p. occurred near 2 nA (7-day-old animal).

Dorsal root stimulation also elicited disynaptic 'direct' i.p.s.p.s (Eccles, 1957). Recurrent inhibitory potentials (Renshaw, 1941) were also recorded following ventral root stimulation, but in most cases were masked by the antidromic spike. In a few cells, failure of antidromic invasion allowed examination of pure recurrent i.p.s.p.s. Both 'direct' and recurrent i.p.s.p.s could be reversed in sign readily by hyperpolarizing current injection. The reversal of a recurrent i.p.s.p. is illustrated in Fig. 10*A*. In order to visualize the synaptic potential clearly, the extracellular field potential has been subtracted from all responses except that obtained at 2 nA (recorded near the reversal point for this i.p.s.p.). The i.p.s.p. amplitude as a function of injected current for three trials in this motoneurone is plotted in Fig. 10*B*. The current required to reverse recurrent i.p.s.p.s (near 2 nA) was similar to that required for the 'direct' i.p.s.p.s, indicating that the two types of inhibitory synapse are similarly located, at least with respect to the length constant of the motoneurones (cf. Burke, Fedina & Lundberg, 1971). If KCl electrodes were used to record from motoneurones (see Burke & Rudomin, 1977) recurrent i.p.s.p.s were seen as hyperpolarizations only immediately following penetration, reversing rapidly to become depolarizing potentials as chloride ions leaked into the cell.

Direct stimulation

Depolarization of neonatal motoneurones with short (about 100 ms), low amplitude outward current pulses elicited responses typical of a passive membrane as shown in Figs. 6*A*, and 11*A*. At threshold for a fast action potential, the spike came from a slow depolarizing prepotential (Fig. 11*A–C*). It is consistent with the high input

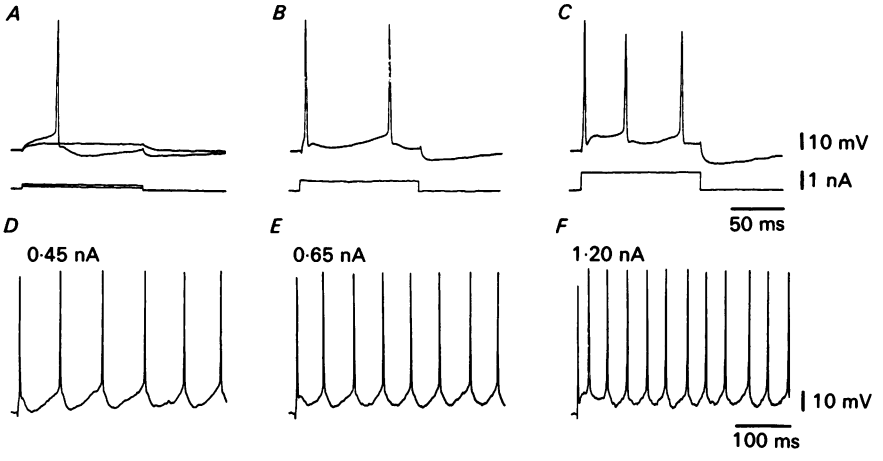

Fig. 11. Direct stimulation of neonatal motoneurones. *A*, subthreshold and threshold current for spike initiation. At threshold a fast spike rises from a slow depolarizing potential and is followed by an a.d.p. and a.h.p. *B* and *C*, increased current injection elicits a second and third spike from slow depolarizations. *D–F*, response of neonatal motoneurones to long current pulses (recorded from another animal). Response to increasing levels of current injection, current amplitude is given on the upper left of each trace. Note decreasing interspike interval as the level of injected current is increased until in *F* at 1·2 nA, a second 'extra' spike rises from the a.d.p. (8-day-old animals.)

resistance of these cells that the amount of current required to reach the firing threshold is considerably less than in adult rat motoneurones (Granit *et al.* 1963*b*). In younger animals (4–6 days old) small spike-like responses were seen on the a.d.p. The ionic dependency and origin of these are considered elsewhere (Walton & Fulton, 1985).

The a.d.p. was succeeded by an a.h.p. which could be close to 200 ms long and extend beyond the end of the pulse (Fig. 11*A–C*). This is in contrast to the adult rat where a.h.p.s of 30–75 ms are typical (Bradley & Somjen, 1961). With further depolarization (Fig. 11*B* and *C*), the trajectory following the spike became steeper and a second spike was elicited at the same threshold as the first. The rate at which the membrane reached the threshold for the second spike increased with current injection decreasing the spike interval (cf. Calvin, 1975). In this cell the threshold for the third spike was lower than that for the others (Fig. 11*C*). In adult rat later spikes have a higher threshold than the first (Bradley & Somjen, 1961).

The membrane also exhibited a subthreshold non-linear response during outward current injection. This was characterized by a slowly rising depolarization followed

by a less pronounced hyperpolarization. This response was dependent on membrane potential, being enhanced by membrane depolarization and diminished by hyperpolarization. This response was similar to that seen in cat motoneurones with natural stimulation (Kolmodin & Skoglund, 1958) but was an order of magnitude larger than the late a.d.p. reported by Eccles, Eccles & Lundberg (1958).

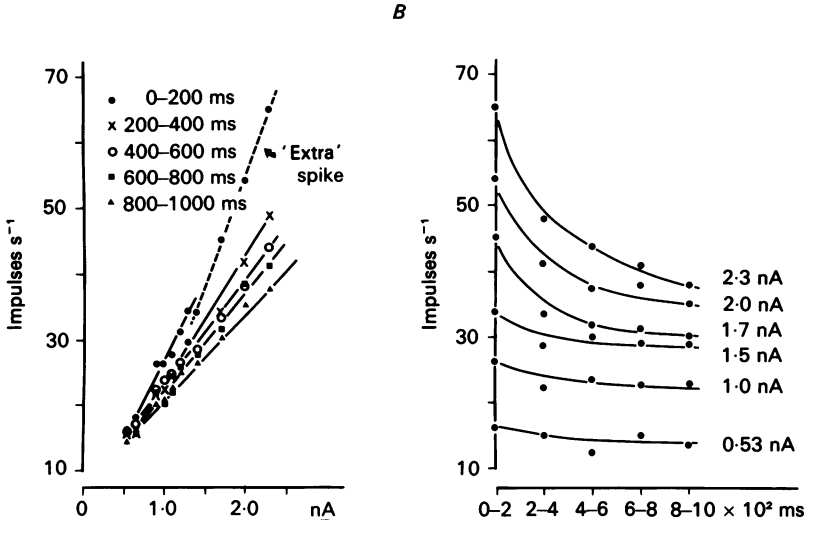

Fig. 12. Repetitive firing characteristics of neonatal motoneurones. *A*, plot of firing frequency as a function of injected current (*f–I*) for five 200 ms time periods following the onset of current injection. The slope of the *f–I* plot increases from the first (0–200 ms, filled circles, slope 23·1 impulses s^{-1} nA^{-1}) to the last (800–1000 ms, triangles, slope 13·4 impulses s^{-1} nA^{-1}) period. Note that the slope for the first period increases when the 'extra' spike is elicited (dashed line, slope 34·4 impulses s^{-1} nA^{-1}). *B*, plot of motoneurone firing frequency as a function of 200 ms time periods following the beginning of the current injection for six current levels. Note that the firing adapts during prolonged current injection and adaptation is complete at the lower current levels by 500 ms. (Same cell as in Fig. 11 *D–F*.)

Stimulation with long current pulses

When cells were activated using long (1–5 s) current pulses 'tonic' but not 'phasic' firing was elicited (Figs. 11 *D–F* and 12; Table 2). Analysis of repetitive firing in the youngest animals (3–6-days-old) was hampered by two factors. It was difficult to establish a clear threshold for continuous firing and, when achieved, the duration of the interspike intervals varied. When consistent firing was seen the relative amplitude of the first few spikes in a series demonstrated two general patterns. In some cells, as in Fig. 11 *B* and *C*, the first spike had the most consistent and largest amplitude, the second spike being about 80 % of the first, and the third and even fourth spikes as low as 60 % of the first. This phenomenon was especially noticeable at high firing frequencies where the first and second interspike intervals were short and presumably results from the conductance underlying the a.h.p. acting as a current shunt. Another

pattern is shown in Fig. 11*D–F* where the response during the first 400 ms of a 1000 ms current pulse is shown. Here the spike height was more consistent, especially at low current levels. In adult rat motoneurones spikes have a constant height except at the highest current levels (Bradley & Somjen, 1961; Granit, Kernell & Shortess, 1963*a*).

TABLE 2. Values for threshold, maximum and minimum firing frequency and gain of the *f–I* plot for several interspike intervals including adapted firing in neonatal motoneurones

Age (days)	Interval	Threshold (nA)	Frequency Min. (Hz)	Frequency Max. (Hz)	Gain of *f–I* plot (impulses s^{-1} nA^{-1})
3	First	1·6	9	40	15·6
	(With 'extra spike')	(3·4)	(94)	(167)	(47)
	Third	2·5	20	29	8·4
5	First	1·4	10	40	20
	(With 'extra spike')	(2·6)	(60)	(125)	(108)
5	First	0·8	8	25	33
	(With 'extra spike')	(1·4)	(36)	(50)	(143)
	Second	0·85	5	29	31
	Third	0·9	7	24	29
5	Adapted	2·3	16	40	12
5	First	2·0	10	38	39·5
	Fourth	2·8	20	35	19
	Fifth	3·2	26	35	19
7	First	1·8	13	32	15
	Second	2·5	17	31	27
8	First	3·7	5	32	12·7
	(With 'extra spike')	(5·5)	(80)	(111)	(33·6)
	Fourth	4·4	12	22	13·3
9	First	2·6	12	30	9·8
	Adapted	3·3	13	30	7·7
10	First	0·23	11	44	59
	(With 'extra spike')	(0·9)	(57)	(68)	—
11	First	0·4	6	19	15
Mean ±S.D.	First	1·6±1·0 (n = 9)	9·3±2·5 (n = 9)	33±7·6 (n = 9)	24·2±15·4 (n = 9)
	(With 'extra spike')	2·8±1·6 (n = 6)	65·4±20 (n = 5)	104±42 (n = 5)	82·9±44·6 (n = 4)

The amplitude of the spike after-potentials varied among the spikes in a train. The first spike had a clear a.d.p. and a.h.p. while the a.d.p. of subsequent spikes was less clearly delineated, although it could often be identified in the next four to six spikes. Subsequent spikes can have a larger a.h.p. than the first, depending on the interspike interval. Spikes occurring toward the end of the current pulse were followed directly by an a.h.p. as in cat motoneurones (Eccles, 1957; Granit *et al.* 1963*a*). This pattern

of decreasing a.d.p. and increasing a.h.p. was identical to that reported by Granit *et al.* (1963*b*) in the adult rat. Note that at a certain level of current an 'extra' spike was generated from the a.d.p. (Fig. 11*F*). Extra spikes were seen to arise from the a.d.p. of the first spike, but not after subsequent spikes, as seen in other types of motoneurones (e.g. Calvin, 1975).

As in the adult rat, the relation between firing frequency and current strength was close to linear (Fig. 12*A*) with one firing range. The mean firing frequencies during successive 200 ms intervals for the cell shown in Fig. 11*D–F* are plotted as a function of injected current (*f–I* plot) in Fig. 12*A*. The sensitivity of the firing rate to injected current decreased with time during the pulse, as reflected in the decreasing slope of the *f–I* plots. This adaptation to current injection (Bradley & Somjen, 1961; Granit *et al.* 1963*b*) is illustrated in Fig. 12*B* where the mean firing frequency as a function of successive 200 ms time intervals is plotted for six current levels. The clearest adaptation was seen at the three highest currents where the firing frequency decreased markedly during the current pulse. At high current levels a large measure of adaptation occurred within 400 ms but was not complete by 1000 ms. At the lower currents adaptation was complete by about 500 ms. Similar (Granit *et al.* 1963*a*) as well as faster (Kernell, 1965*a*) adaptation rates have been reported for adult rat motoneurones.

A secondary range of firing typically seen in cat motoneurones (Kernell, 1965*a*) was not seen. This was not due to insufficient current injection since inactivation of the firing mechanism was observed at the highest current levels used. An apparent secondary firing range was seen during the first 200 ms (dashed line, Fig. 12*A*). This occurred, however, only when 'extra' spikes were generated from the a.d.p. Further, these two apparent ranges overlap (near 30 Hz, Fig. 11*A*), while there is a break between the primary and secondary ranges in cat motoneurones (Kernell, 1965*a*; Calvin, 1975).

DISCUSSION

We have used an *in vitro* preparation to study the electroresponsive properties of neonatal rat motoneurones using both extracellular and intracellular recording techniques. The results indicate that no significant loss of tissue viability or tissue distortion occurred as a result of the isolation and hemisection of the spinal cord. On this basis we consider it valid to compare motoneurone behaviour in this preparation with that observed *in vivo*.

Extracellular field potentials

By monitoring the field potentials the behaviour of specific neuronal populations in the ventral motor area (following antidromic invasion) and in the entire hemicord (following dorsal root stimulation) has been studied. This is the first study of such fields in this preparation and the results indicate that current sources and sinks correspond to anatomically defined pathways and cell populations of new-born mammals (see Cajal, 1911; Stelzner, 1971). Such a study may be especially relevant in determining when synaptic contacts, known to be present from morphological studies, are capable of eliciting post-synaptic responses. For, although the times of

arrival of dorsal root and descending (Stelzner, 1971; Gilbert & Stelzner, 1979) inputs have been determined in morphological studies, whether these contacts are functional at these times is largely unknown. The region where the large amplitude negative component of the orthodromic field potential is dominant (Fig. 4) corresponds to the nucleus proprius of the adult (lamina IV of Rexed (1954)), and to the intermediate and dorsomedial zone described by Stelzner (1971) in neonatal rats. Dorsal root fibres make extensive connexions to these areas, including monosynaptic connexions from I a and I b fibres (Cajal, 1911; Sprague & Ha, 1964) and in electrophysiological studies in cat spinal cord, the maximum amplitude extracellular response generated by group I a and I b fibres of biceps semitendinosus nerve (Eccles *et al.* 1954) was recorded here as were intracellular responses from interneurones (Eccles, Eccles & Lundberg, 1960). Our extracellularly recorded potentials appear to coincide with the location of greatest synaptic density (cf. Eccles *et al.* 1954) and the large negative responses shown in Fig. 4 presumably reflect the synaptic activation of interneurones. The presence of this field in a 7-day-old animal indicates that the stained synaptic end-feet described by Stelzner (1971) to be densely argyrophilic at this age are in fact functional, at least in terms of eliciting post-synaptic responses in the interneurones. Thus, the field potential recordings provide insight into the sites of current sources and sinks and which cell populations can be activated by anatomically defined synaptic contacts during post-natal development.

Characteristics of individual motoneurones

The electrophysiological characteristics of individual neonatal motoneurones were, in many respects, similar to those of adult motoneurones studied *in vivo*. There are, however, some obvious points of difference which merit discussion.

Passive properties. The input resistances we have observed are much higher than those reported for adult rat motoneurones, as with kitten motoneurones compared to cat (Shapovalov *et al.* 1981). Since motoneurones are known to grow considerably after birth (Mellstrom & Skoglund, 1969; Conradi, 1976) it is likely that the high input resistance is a consequence of the small size of these cells. Variation of input resistance with cell size is expected from theoretical considerations (Rall, 1977) and confirmed by measurements made from adult cat motoneurones (Kernell, 1966), however, see Kernell & Zwaagstra (1981). Our own measurements confirm that over the post-natal period studied the soma size increases steadily; we estimate the surface area of the soma to increase from 1300 μm^2 at 1 day to 2550 μm^2 at 9 days after birth. During this period we have seen a concomitant decrease in input resistance from a high near 30 MΩ to a low near 4 MΩ. However, it is unlikely that soma size is the sole contributory factor (cf. Gustafsson & Pinter, 1984) as changes in dendritic configuration and dimensions also occur (Conradi, 1976). The measured values for membrane time constant fall within those for adult cat (Eccles, 1957).

Action potentials. Although the spikes recorded from neonatal rat spinal motoneurones are similar in many respects to those seen in prenatal (Naka, 1964) and post-natal kitten (Kellerth *et al.* 1971), they differ in having prominent after-potentials. In fact, in fetal cat (Naka, 1964) after-potentials were seen only in injured cells or in the second response of a pair of stimuli. The reliability and prominence of the a.d.p. in neonatal rat also contrasts with adult rat motoneurones where the a.d.p. is not

always elicited (Granit *et al.* 1963*b*; Kernell, 1964). There are several, not mutually exclusive, explanations for the prominence of this component in neonatal rat motoneurones. (1) The mechanical stability of the *in vitro* preparation may allow cells to be penetrated without injury more readily than *in vivo* and thus the a.d.p. is more reliably recorded. (2) If, as has been suggested (Granit *et al.* 1963*b*; Kernell, 1964; Nelson & Burke, 1967) the conductance underlying the a.d.p. is located away from the somatic recording site in the dendrites, then the potential recorded in the soma would be larger in the neonate than in the adult due to the high input resistance and decreased effective space constant of neonatal motoneurones. (3) The conductance underlying the a.d.p. may simply be larger in neonatal motoneurones. Thus this event, whether dendritic, somatic or both, is more prominent in developing cells.

The a.h.p. of neonatal rat motoneurones is quite prolonged with a range of 65–178 ms. This is in contrast to the brief a.h.p.s of adult rat which last 30–75 ms (Bradley & Somjen, 1961) and become prominent only during repetitive firing (Granit *et al.* 1963*b*). Although no single parameter is sufficient, a.h.p. duration is often used to distinguish motoneurones innervating fast twitch from those innervating slow twitch muscle fibres (cf. Burke & Rudomin, 1977), the a.h.p. being longer in slow-twitch type motoneurones. The long duration of the a.h.p. with respect to the adult suggests that neonatal motoneurones, during the period investigated in this study (up to 12 days old), are of the slow-twitch type. By contrast, in 16–20-day-old kittens the a.h.p.s of both medial gastrocnemius (fast-twitch type) and soleus (slow-twitch type) α-motoneurones were reported to be short (near 60 ms), the a.h.p. duration of soleus motoneurones increasing with development (to near 150 ms), while that of the gastrocnemius remained relatively constant (Huizar, Kuno & Miyata, 1975). Studies of neonatal rat motoneurones identified by muscle type are required to investigate this apparent difference between kitten and neonatal rat motoneurones.

As in other preparations, the shape of the action potential is very sensitive to membrane potential level. While hyperpolarization of the membrane showed the action potential to comprise s.d., i.s. and M components as in the adult motoneurones (Brock *et al.* 1953; Coombs *et al.* 1955), less current was required to prevent both s.d. and i.s. invasion in the neonatal cells. This probably results partly from the higher input resistance. In the cat the diameter of the motoneurone initial segment at birth is about half of that in the adult animal (Conradi, 1976), which would result in a lowered safety factor for antidromic invasion in the neonate (Kellerth *et al.* 1971). However, we found that the antidromic spike succeeded in invading the soma in a significant majority of cells; failure occurring in less than 5 % of the cases. Failure of antidromic invasion often occurs in injured cells and reliability of invasion in this study as compared to others (Naka, 1964; Kellerth *et al.* 1971) may simply be due to the greater mechanical stability of the isolated preparation.

When motoneurones were hyperpolarized sufficiently to prevent invasion of the spike into the s.d. compartment, the a.d.p. and a.h.p. were no longer present. The apparent dependence of these after-potentials on the presence of s.d. invasion indicates that they are generated across this portion of the cell membrane (Granit *et al.* 1963*b*; Kernell, 1964; Nelson & Burke, 1967) rather than in the initial segment. This is clear when the i.s. spike is directly compared to the partial spike elicited from

a depolarized level (Fig. 10*C*). The delineation of the site of origin of the latter spike to soma or dendrite cannot be made on the basis of the present results.

Synaptic potentials. We have demonstrated that in some cells the composite Ia e.p.s.p. can be completely and readily reversed by injected current. We observed two types of e.p.s.p.: those with a biphasic (rising phase first) reversal of the kind reported for climbing fibre e.p.s.p.s in cerebellar Purkinje cells (Llinás & Nicholson, 1976) and in some pools of cat motoneurones (cf. Eccles, 1957), and others in which the early phase was relatively unaffected by current injection. Although our sample size is small, we have not observed a single e.p.s.p. in which the latter portion of the potential reversed at a lower level of injected current than the early portion. This is in contrast with most *in vivo* cat studies (cf. Redman, 1979).

The reversal of the rising phase of the e.p.s.p. with lower levels of injected current than the latter phase probably reflects the distribution of Ia synapses (Terzuolo & Llinás, 1966). Those close to the site of current injection (presumably the soma) contribute to the rising phase of the e.p.s.p. and are reversed with the least current, while those further away (presumably on the dendrites) require more current for their reversal. The relative ease with which the entire e.p.s.p. can be reversed in these immature cells may be related to small size and high input resistance. Developmental differences in the distribution of Ia synapses may also be a contributing factor (Gilbert & Stelzner, 1979). The current-insensitive early phase of some e.p.s.p.s may be explained by the occurrence of a synaptically evoked regenerative phenomenon, such as dendritic spiking (cf. Llinás, 1984). They may correspond to the prepotentials ('local response') seen by Naka (1964) in fetal and new-born cat. The properties of e.p.s.p.s in this preparation are under further investigation (Walton, 1984).

In contrast with excitatory potentials, i.p.s.p.s were, without exception, reversed by current injection as well as by intracellular injection of chloride ions. In cat motoneurones recurrent i.p.s.p.s do not reverse readily with injection of chloride ions (cf. Burke & Rudomin, 1971). It is unlikely that the ionic mechanisms underlying i.p.s.p.s in cat and neonatal rat are different. Rather the sensitivity seen in the rat may be due to the relatively small volume of the soma facilitating a greater increase in intracellular chloride ion concentration.

Activation of motoneurones with injected current. The characteristics of repetitive firing in neonatal motoneurones (summarized in Table 2) raise four points of interest with respect to those of adult cells. (1) There does not always appear to be a threshold for maintained firing and the interspike interval can be quite variable. This is especially prominent in the youngest animals studied (3–6 days old). (2) The maximum firing rates are low (33 Hz, S.D. $\pm$7·6 Hz) compared to adult rat (100–180 Hz; Bradley & Somjen, 1961; Granit *et al.* 1963*a*). (3) The gain of the *f–I* plot is high compared to the adult (Granit *et al.* 1963*a*). (4) The time course of adaptation appears to be longer than that in adult motoneurones. Because of its relation to the development of muscle tensile strength this is an especially important parameter in understanding the development of the neuromuscular system and requires further study.

The lack of a threshold for repetitive firing and the variability in interspike intervals are consistent with electromyographic studies in new-born rats. Bursian

(1971) found the tonic response to stretch of the gastrocnemius muscle to be absent at birth, the duration of firing slowly developing from a single spike to a train during the first two post-natal weeks. Furthermore, there was no correlation between motor unit discharge frequency and muscle tension until two weeks after birth (Bursian & Sviderskaya, 1971). During the same post-natal period Navarrete & Vrbová (1983) found a decrease in the variability of interspike intervals in motor units. The setting of a threshold for repetitive firing and the establishment of a constant firing rate thus occur as part of the developmental sequence of the organization of the neuromuscular system.

The second finding, of a low maximum firing rate, is probably related to the prolonged a.h.p. seen in these cells (Table 1) compared to adult animals and is consistent with the report in rat and cat that motor unit firing rate is initially low in neonates but increases during post-natal development (Bursian, 1971; Bursian & Sviderskaya, 1971; but see Huizar *et al.* 1975). It has been established that all limb muscles are equally slow at birth and in the rat differentiation into fast and slow types does not occur until the second to third post-natal week (Close, 1964). The differentiation between tonic and phasic motoneurones is likewise not established at birth (Eccles *et al.* 1958). The low firing frequency observed here may thus reflect a resonance between the properties of the neonatal motoneuronal and muscular systems. Indeed, the optimum frequency for repetitive stimulation of rat muscle is low at birth and increases post-natally (Close, 1964). The firing properties of motoneurones in neonates may be matched not only to muscle contractile properties, but also to the release characteristics of the neuromuscular junctions. End-plate potentials of embryonic rat muscle initially have a low quantal content which increases with development (Dennis, Ziskind-Conhaim & Harris, 1981). A corollary of this low quantal content would be an inability of the junction to follow repetitive stimulation (Letinsky, 1974). The findings of Huizar *et al.* (1975) indicate a degree of independence between a.h.p. duration, and muscle contractile properties in kittens, although they did not define the relation between motoneurone discharge patterns and muscle contractile properties.

Low frequency firing in neonates compared to adults has also been found in sensory systems. The maximum firing frequency of dorsal column nuclei cells is three times higher in cats than in kittens (Connor, Ferrington & Rowe, 1984). A similar pattern is seen in afferent fibres to the cuneate nucleus (Ferrington & Rowe, 1980) and neurones of the vestibular system (Lannou, Precht & Cazin, 1979). Thus, in sensory and motor systems both central and peripheral components exhibit a slower rate of firing accompanied by a less accurate representation of sensation and execution of movement in neonates as compared to adults. This has been demonstrated clearly in behavioural studies of locomotion (Stelzner, 1971; cf. Navarrete & Vrbová, 1983). The mechanisms underlying this slow rate of firing are discussed elsewhere (Walton & Fulton, 1985).

The third point, concerning the high gain of the *f–I* plot, brings up the question of whether this single firing range is best compared with the primary or secondary range typical of cat motoneurones (Kernell, 1965*a*). The second range observed at short intervals in the presence of 'extra' spikes in neonatal cells (dashed line, Fig. 12*A*) cannot be considered as a true second firing range and will therefore not be

considered further here. In addition to their dependency on the current level, primary and secondary range firing can be distinguished by the maximum firing rate, the slope of the *f–I* plot, and the spike after-potential trajectories (Kernell, 1965*a*, *b*; Calvin, 1975; Heyer & Llinás, 1977). Regarding firing frequency, steady-state firing in the neonatal rat demonstrates a maximum rate of 33 Hz (S.D. = ±7·6) with a range of 19–44 Hz, values which fall at the lower end of the primary range in cat (mean 51, S.D. = ±17 Hz, range 30–75 Hz; Kernell, 1965*a*), and well below the maximum firing frequency of adult rat (100–180 Hz, Granit *et al.* 1963*a*). In fact, adult rat values fall within the secondary range of cat (125 Hz, S.D. = ±38, range 88–125 Hz; Kernell, 1965*a*). The latter is consistent with the observation that the a.h.p. following a single spike in adult rat is shorter than that in adult cat (Bradley & Somjen, 1961). So, by this criterion neonatal rat firing falls within the primary range while that of adult rat falls within the secondary range of the cat.

The slope (gain) of the *f–I* plot of neonatal rat for both 'instantaneous' and adapted firing (Table 2) is higher than those for the secondary range in cat (2·7–6·7 impulses s^{-1} nA^{-1}, Kernell, 1965*a*; 6·8 impulses s^{-1} nA^{-1}, Heyer & Llinás, 1977). Again, adult rat has secondary range characteristics (4–6 impulses s^{-1} nA^{-1}, Granit *et al.* 1963*a*). Since the *f–I* plot gain is affected by the cell size (Henneman, Somjen & Carpenter, 1965) and thus by input resistance (Kernell, 1966), the latter may contribute to the high gain values in the neonate. Finally, the post-spike trajectories of neonatal motoneurones during repetitive firing are typical of cat primary range firing (Calvin, 1975; Heyer & Llinás, 1977), as are those of adult rat motoneurones. Thus, by two of the three characteristics, maximum firing rate and trajectory, firing in neonatal motoneurones appears to correspond more closely to the primary than to the secondary range identified in cat spinal motoneurones.

This raises the question of the mechanisms which underlie secondary range firing and the reason for its absence in neonatal rat. It was proposed long ago that motoneurone firing is controlled by the hyperpolarization which follows each spike (Eccles, 1936). Although this is certainly the case in neonatal motoneurones, it can be argued that in these cells the a.h.p. is secondary to the a.d.p. in this respect, the duration of the a.h.p. being directly related to the amplitude of the a.d.p. (Fig. 7) (Harada & Takahashi, 1983; Walton & Fulton, 1985). The prominent a.d.p. together with the subsequent a.h.p. may thus prevent high frequency firing. Indeed, if the a.h.p. is bypassed, as occurs when an extra spike is generated from the a.d.p., neonatal motoneurones fire at 'instantaneous' rates as high as 100 Hz (Table 2). Thus, the a.h.p. would prevent secondary range firing in these cells if the conductance increase underlying the a.h.p. causes a significant current shunt. The membrane potential level at which the s.d. component of the second of a pair of antidromic spikes failed, was less negative than that for failure during direct membrane hyperpolarization indicating the presence of a strong conductance increase during the a.h.p.

On the basis that the a.d.p. and a.h.p. are due to invasion of the action potential into dendrites, Granit and his colleagues (Granit, Kernell & Lamarre, 1966) proposed that secondary range firing was due to inactivation of the dendritic conductances and thus elimination of the a.d.p. (and a.h.p.). If this were to be the case, and if the dendritic depolarization and the a.h.p. it triggers is robust in neonates, one would expect the dendrites to be resistant to inactivation and secondary range firing would

be absent. There is experimental evidence that an increased conductance to calcium underlies the a.d.p. in neonatal motoneurones and that both a voltage- and calcium-dependent potassium conductance underlie the a.h.p. (Harada & Takahashi, 1981, 1983; Fulton & Walton, 1981; Walton & Fulton, 1985). Thus these three conductances, through their strength and location in the motoneurone membrane could prevent secondary range firing in neonatal motoneurones. The control of repetitive firing and its ionic basis is discussed further elsewhere (Walton & Fulton, 1985).

We would like to thank Professor Ricardo Miledi for his hospitality during the beginning of these experiments at University College London. We are specially indebted to Professor Rodolfo Llinás for his continued advice and helpful criticism during the completion of the experiments and preparation of the manuscript at New York University. Research was supported by The Medical Research Council, and United States Public Health Service Fellowship NS-06275 and program grant NS-13742 from the National Institute of Neurological and Communicative Disorders and Stroke.

REFERENCES

BAGUST, J. & KERKUT, G. A. (1981). An *in vitro* preparation of the spinal cord of the mouse. In *Electrophysiology of Isolated Mammalian CNS Preparations*, ed. KERKUT, G. A. & WHEAL, H. V., pp. 337–365. New York: Academic Press.

BRADLEY, K. & SOMJEN, G. G. (1961). Accommodation in motoneurones of the rat and the cat. *Journal of Physiology* **156**, 75–92.

BROCK, L. G., COOMBS, J. S. & ECCLES, J. C. (1952). The recording of potentials from motoneurones with an intracellular electrode. *Journal of Physiology* **117**, 431–460.

BROCK, L. G., COOMBS, J. S. & ECCLES, J. C. (1953). Intracellular recording from antidromically activated motoneurones. *Journal of Physiology* **122**, 429–461.

BURKE, R. E., FEDINA, L. & LUNDBERG, A. (1971). Spatial synaptic distribution of recurrent and group IA inhibitory systems in cat spinal motoneurones. *Journal of Physiology* **214**, 305–326.

BURKE, R. E. & RUDOMIN, P. (1977). Spinal neurons and synapses. In *The Handbook of Physiology*, section I, *The Nervous System*, vol. I, *Cellular Biology of Neurons*, part 2, ed. BROOKHART, J. M. & MOUNTCASTLE, V. B., pp. 877–944. Bethesda: American Physiological Society.

BURSIAN, A. V. (1971). The development of the stretch reflex in young rats. *Journal of Evolutionary Biochemistry and Physiology* **9**, 525–529.

BURSIAN, A. V. & SVIDERSKAYA, G. E. (1971). Studies on the the activity of motor units in newborn rats and kittens. *Journal of Evolutionary Biochemistry and Physiology* **7**, 255–261.

CAJAL, S. (1911). *Histologie du System Nerveux de l'Homme et des Vertebres*, vol. I. Madrid: Instituto Ramon Y Cajal.

CALVIN, W. H. (1975). Generation of spike trains in CNS neurons. *Brain Research* **84**, 1–22.

CLOSE, R. (1964). Dynamic properties of fast and slow skeletal muscles of the rat during development. *Journal of Physiology* **173**, 74–95.

CONNOR, M., FERRINGTON, D. G. & ROWE, M. J. (1984). Tactile sensory coding during development: signaling capacities of neurons in kitten dorsal column nuclei. *Journal of Neurophysiology* **52**, 86–98.

CONRADI, S. (1976). Functional anatomy of the anterior horn motor neuron. In *The Peripheral Nerve*, ed. LANDON, D. N., pp. 279–329. London: Chapman and Hall.

COOMBS, J. S., ECCLES, J. C. & FATT, P. (1955). The electrical properties of the motoneurone membrane. *Journal of Physiology* **130**, 291–325.

DENNIS, M. J., ZISKIND-CONHAIM, L. & HARRIS, A. J. (1981). Development of neuromuscular junctions in rat embryos. *Developmental Biology* **81**, 266–279.

ECCLES, J. C. (1936). Synaptic and neuromuscular transmission. *Ergebnisse der Physiology* **38**, 339–444.

ECCLES, J. C. (1957). *The Physiology of Nerve Cells*. Baltimore: The Johns Hopkins Press.

ECCLES, J. C., ECCLES, R. M. & LUNDBERG, A. (1958). The action potentials of the alpha motoneurones supplying fast and slow muscles. *Journal of Physiology* **142**, 275–291.

ECCLES, J. C., ECCLES, R. M. & LUNDBERG, A. (1960). Types of neurone in and around the intermediate nucleus of the lumbosacral cord. *Journal of Physiology* **154**, 89–114.

ECCLES, J. C., FATT, P., LANDGREN, S. & WINSBURY, G. J. (1954). Spinal cord potentials generated by volleys in the large muscle afferents. *Journal of Physiology* **125**, 590–606.

FERRINGTON, D. G. & ROWE, M. J. (1980). Functional capacities of tactile afferent fibres in neonatal kittens. *Journal of Physiology* **307**, 335–353.

FULTON, B. P. (1983). Motoneurone activity in an *in vitro* preparation of adult mammalian spinal cord. *Journal of Physiology* **342**, 64–65*P*.

FULTON, B. P. & WALTON, K. (1981). Calcium dependent spikes in neonatal rat spinal cord *in vitro*. *Journal of Physiology* **317**, 25–26*P*.

GILBERT, M. & STELZNER, D. J. (1979). The development of descending and dorsal root connections in the lumbosacral spinal cord of the postnatal rat. *Journal of Comparative Neurology* **184**, 821–838.

GRANIT, R., KERNELL, D. & LAMARRE, Y. (1966). Synaptic stimulation superimposed on motoneurones firing in the 'secondary' range to injected current. *Journal of Physiology* **187**, 401–415.

GRANIT, R., KERNELL, D. & SHORTESS, G. K. (1963*a*). Quantitative aspects of repetitive firing of mammalian motoneurone, caused by injected current. *Journal of Physiology* **168**, 911–931.

GRANIT, R., KERNELL, D. & SMITH, R. S. (1963*b*). Delayed depolarization and the repetitive response to intracellular stimulation of mammalian motoneurones. *Journal of Physiology* **168**, 890–910.

GUSTAFSSON, B. & PINTER, M. J. (1984). Relations among passive electrical properties of lumbar α-motoneurones of the cat. *Journal of Physiology* **356**, 401–431.

HARADA, Y. & TAKAHASHI, T. (1981). Calcium spike in the mammalian spinal motoneuron. *Proceedings of the Japan Academy* **57**(B), 394–397.

HARADA, Y. & TAKAHASHI, T. (1983). The calcium component of the action potential in spinal motoneurones of the rat. *Journal of Physiology* **325**, 89–100.

HENNEMAN, E., SOMJEN, F. G. & CARPENTER, D. O. (1965). Functional significance of cell size in spinal motor neurones. *Journal of Neurophysiology* **28**, 560–580.

HEYER, C. B. & LLINAS, R. (1977). Control of rhythmic firing in normal and axotomized cat spinal motoneurones. *Journal of Neurophysiology* **40**, 480–488.

HUIZAR, P., KUNO, M. & MIYATA, Y. (1975). Differentiation of motoneurones and skeletal muscles in kittens. *Journal of Physiology* **252**, 465–479.

KELLERTH, J-O., MELLSTROM, A. & SKOGLUND, S. (1971). Postnatal excitability changes of kitten motoneurones. *Acta physiologica scandinavica* **83**, 31–41.

KERNELL, D. (1964). The delayed depolarization in cat and rat motoneurones. *Progress in Brain Research* **12**, 42–55.

KERNELL, D. (1965*a*). High-frequency repetitive firing of cat lumbosacral motoneurones stimulated by long-lasting injected currents. *Acta physiologica scandinavica* **65**, 74–86.

KERNELL, D. (1965*b*). The limits of firing frequency in cat lumbosacral motoneurones possessing different time course of afterhyperpolarization. *Acta physiologica scandinavica* **65**, 87–100.

KERNELL, D. (1966). Input resistance, electrical excitability and size of ventral horn cells in cat spinal cord. *Science* **152**, 1637–1640.

KERNELL, D. & ZWAAGSTRA, B. (1981). Input conductance, axonal conduction velocity and cell size among hindlimb motoneurones of the cat. *Brain Research* **204**, 311–326.

KOLMODIN, G. M. & SKOGLUND, C. R. (1958). Slow membrane potential changes accompanying excitation and inhibition in spinal moto- and interneurons in the cat during natural activation. *Acta physiologica scandinavica* **44**, 11–54.

LANNOU, J., PRECHT, W. & CAZIN, L. (1979). The postnatal development of functional properties of central vestibular neurons in the rat. *Brain Research* **175**, 219–232.

LETINSKY, M. S. (1974). Physiological properties of developing tadpole nerve–muscle junctions during repetitive stimulation. *Developmental Biology* **40**, 154–161.

LLINÁS, R. (1984). Comparative electrobiology of mammalian central neurons. In *Brain Slices*, ed. DINGLEDINE, R., pp. 7–23. New York: Plenum Publishing Corporation.

LLINÁS, R. & NICHOLSON, C. (1976). Reversal properties of climbing fiber potential in cat Purkinje cells; an example of a distributed synapse. *Journal of Neurophysiology* **39**, 311–323.

LLINÁS, R. & SUGIMORI, M. (1980). Electrophysiologial properties of *in vitro* Purkinje cell somata in mammalian cerebellar slices. *Journal of Physiology* **305**, 171–195.

LORENTE DE NO, R. (1947). Action potential of the motoneurones of the hypoglossus nucleus. *Journal of Cell and Comparative Physiology* **29**, 207–287.

MELLSTROM, A. & SKOGLUND, S. (1969). Quantitative morphological changes in some spinal cord segments during postnatal development. *Acta physiologica scandinavica*, suppl. **331**.

NAKA, K. (1964). Electrophysiology of the fetal spinal cord. I. Action potentials of the motoneuron. *Journal of General Physiology* **47**, 1003–1022.

NAVARRETE, R. & VRBOVÁ, G. (1983). Changes in activity patterns in slow and fast muscles during postnatal development. *Developmental Brain Research* **8**, 11–19.

NELSON, P. G. & BURKE, R. E. (1967). Delayed depolarization in cat spinal motoneurones. *Experimental Neurology* **17**, 16–26.

NELSON, P. G. & FRANK, K. (1964). Extracellular potential fields of single spinal motoneurones. *Journal of Neurophysiology* **27**, 913–927.

NELSON, P. G. & FRANK, K. (1967). Anomalous rectification in cat spinal motoneurones and effect of polarizing currents on excitatory postsynaptic potential. *Journal of Neurophysiology* **30**, 1097–1113.

OTSUKA, M. & KONISHI, S. (1974). Electrophysiology of mammalian spinal cord *in vitro*. *Nature* **252**, 733–734.

PITTS, W. (1952). Investigations on synaptic transmission. In *Cybernetics*, ed. VON FOERSTER, H., pp. 159–168. New York: Josiah May Foundation.

RALL, W. (1977). Core conductor theory and cable properites of neurons. In *Handbook of Physiology*, section 1, *The Nervous System*, vol. I, *Cellular Biology of Neurons*, part 1, ed. BROOKHART, J. M. & MOUNTCASTLE, V. B. Bethesda: American Physiological Society.

REDMAN, S. (1979). Junctional mechanisms at group Ia synapses. *Progress in Neurobiology* **12**, 33–83.

RENSHAW, B. (1940). Activity in the simplest spinal reflex pathways. *Journal of Neurophysiology*, **3**, 373–387.

RENSHAW, B. (1941). Influence of discharge of motoneurons upon excitation of neighboring motoneurons. *Journal of Neurophysiology* **4**, 167–183.

REXED, B. (1954). A cytoarchitectonic atlas of the spinal cord in the cat. *Journal of Comparative Neurology* **100**, 297–380.

SAITO, K. (1979). Development of spinal reflexes in the rat fetus studied *in vitro*. *Journal of Physiology* **294**, 581–594.

SHAPOVALOV, A. I., SHIRIAEV, B. I. & TAMAROVA, Z. A. (1981). A study of neuronal activity of mammalian superfused or intra-arterially perfused CNS preparations. In *Electrophysiology of Isolated Mammalian CNS Preparations*, ed. KERKUT, G. A. & WHEAL, H. V., pp. 367–394. New York: Academic Press.

SPRAGUE, J. M. & HA, H. (1964). The terminal fields of dorsal root fibers in the lumbosacral spinal cord of the cat, and the dendritic organization of the motor nuclei. *Progress in Brain Research* **11**, 120–154.

STELZNER, D. J. (1971). The normal postnatal development of synaptic end-feet in the lumbosacral spinal cord and of responses in the hind limbs of the albino rat. *Experimental Neurology* **31**, 337–357.

TAKAHASHI, T. (1978). Intracellular recording from visually identified motoneurons in rat spinal cord slices. *Proceedings of the Royal Society* B **202**, 417–421.

TAKAHASHI, T. (1984). Inhibitory miniature synaptic potentials in rat motoneurones. *Proceedings of the Royal Society* B **221**, 103–109.

TERZUOLO, C. A. & LLINÁS, R. (1966). Distribution of synaptic inputs in the spinal motoneurone and its functional significance. In *Muscular Afferents and Motor Control*, ed. GRANIT, R., pp. 373–384. New York: John Wiley & Sons.

WALTON, K. (1984). Reversal properties of monosynaptic e.p.s.p.s in neonatal rat motoneurones studied in spinal cord in vitro. *Society for Neuroscience Abstracts* **10**, 4.

WALTON, K. D. & FULTON, B. P. (1981). Role of calcium conductance in neonatal motoneurones of isolated rat spinal cord. *Society for Neuroscience Abstracts* **7**, 246.

WALTON, K. & FULTON, B. (1983). Hydrogen peroxide as a source of molecular oxygen for *in vitro* mammalian CNS preparations. *Brain Research* **278**, 387–393.

WALTON, K. & FULTON, B. P. (1985). The ionic mechanisms underlying the firing properties of rat neonatal motoneurones studied *in vitro*. *Neuroscience* (in the Press).

WRIGHT, E. B. (1954). Effect of mephenesin and other 'depressants' on spinal cord transmission in frog and cat. *American Journal of Physiology* **179**, 390–401.